Sp converted wave structure imaged by the CREST, SIEDCAR, CDROM, Transportable arrays in Wyoming, Colorado, and New Mexico

Ken Dueker, Steve Hansen, Joe McClenahan; Univ. of Wyoming; *Portland LAB Meeting 8/15/2011*

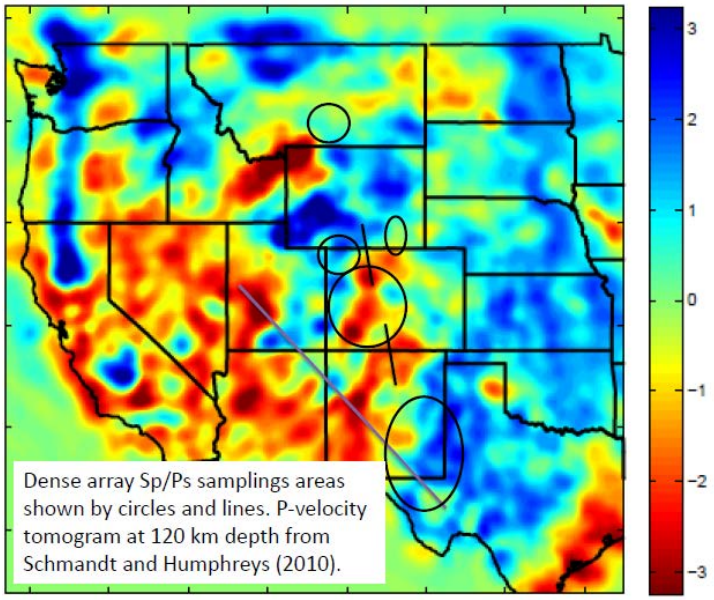

Dense array Sp/Ps samplings areas shown by circles and lines. P-velocity tomogram at 120 km depth from Schmandt and Humphreys (2010).

Introduction. Ps and Sp images of sub-moho negative arrivals beneath the intermountain region of western U.S. are made using dense (2-40 km station spacing) arrays shown to the left that recorded for 1-2 years: the CREST, RISTRA, SIEDCAR, LODORE, LARAMIE, BILLINGS array data combined with Transportable Array data. The nominal Sp interpretational zoo includes an LAB arrival thought to manifest the juxtaposition of melt against the base of the thermal lithosphere and a MLD arrival that manifest a low velocity step/notch in the middle of the chemical lithosphere. Our images find a zoo of sub-moho Sp negative features - namely sharp offsets, doublets, and dim-outs - that sometimes correlate as expected with the upper mantle velocity structure, but sometimes do not. The primary Sp negative arrival is at 70-95 km depth and shallows 20-30 km beneath the Colorado Rocky Mountains (CRM), the Rio Grande Rift (RGR), and at the Basin and Range/Colorado Plateau boundary (BR/CP). A second deeper Sp negative is found at 150-160 km depth in SE New Mexico. The deeper Sp negatives may manifest a deep solidus crossing due to the upwelling of hydrous diapirs from a 410 low-velocity layer imaged by Ps waves beneath the CRM. Interpretation of these Sp features, in tandem with Ps images and surface and body wave tomograms, are helping to constrain the origin (lithospheric potential energy release or upwelling transition zone diapirs) of the positive buoyancy flux required to drive the young (<9 Ma) uplift of this area.

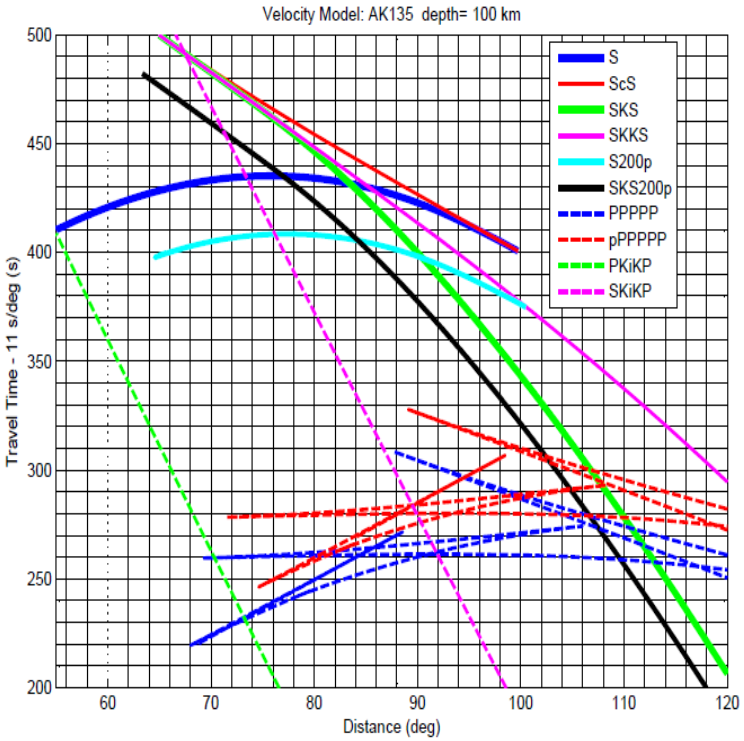

S/SKS P-contamination. Isolation of forward scattered Sp arrivals is complicated by three issues: 1) Post-critical Sp reverberation from the Moho at <54°; 2) About the SKS/S cross-over distance when SKS/S arrivals have comparable magnitude: interference of Sp/SKSp arrivals and isolation of the incident SV-component wavelet; 3) For a 100 km depth event at 102°, the pPPPPP phase crosses the $SKS_{200}p$ phase (Fig. 1). Issue one is solved via delta windowing. Issue two is solved by only using signal about the SKS/S cross-over when one phase is dominant. Issue three is solved by visual identification of pPPPPP arrivals and not using these events (Fig. 2). A P-arrival 25 s before SKS is found with the same waveshape and moveout as the SKS arrival (Fig. 3). This raw arrival is mapped to the negative velocity contrasts beneath the Jemez Volcanic lineament in the Big-Line CCP-image (Fig. 4).

Figure 1. Travel-time plot using AK135 velocity model for 100 km depth source.

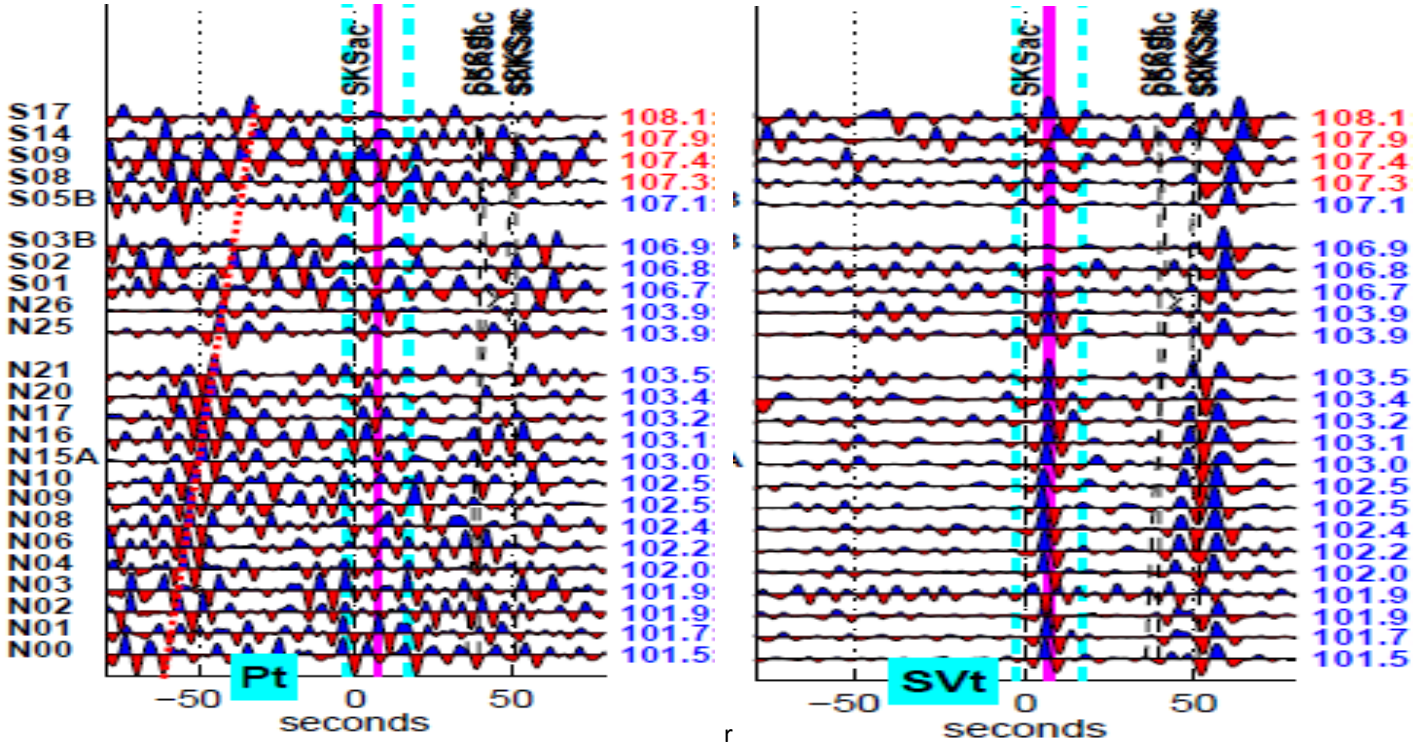

Figure 2. P (left) and SV (right) component recordings from CREST array at 101-108° delta from 6.2 M_b Hindu Kush event at 108 km depth. The red dotted line shows the pPPPPP arrival with prograde moveout with respect to the SKSac arrival; this arrival is a source of Sp arrival pollution.

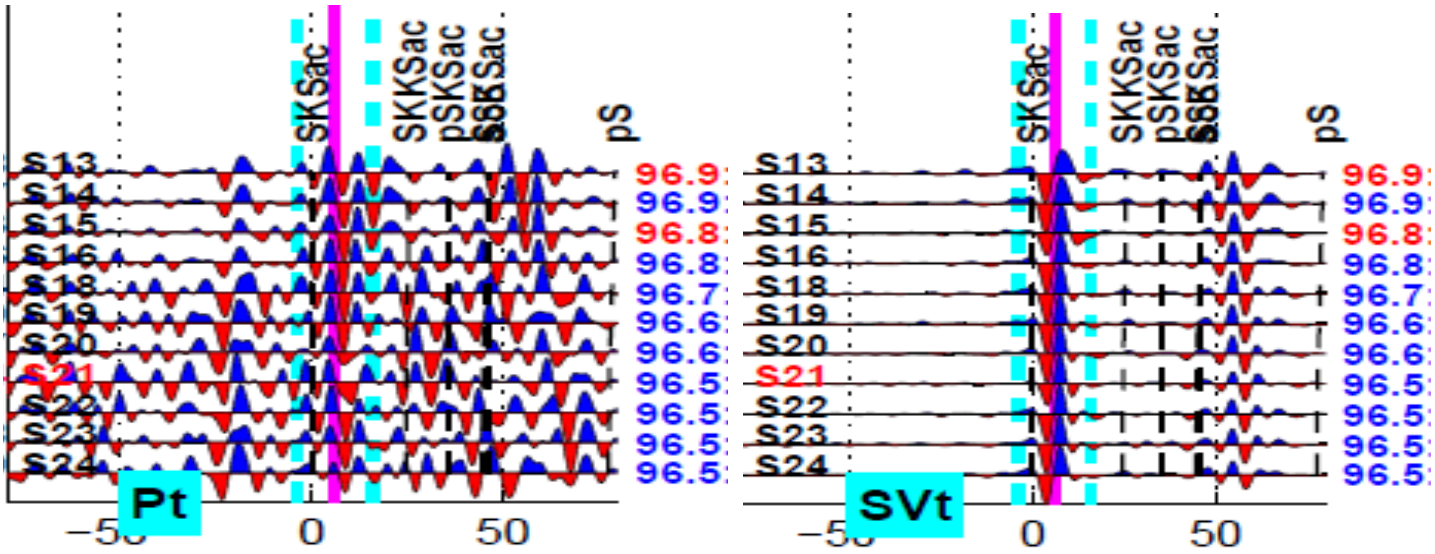

Figure 3. P (left) and SV (right) component recordings from CDROM-south line at 96.5-96.9° offset. Earthquake is 96 km depth M_b 6.2 from Tonga. The P- arrival at -25 s is a S160p arrival with the same polarity and wave-shape at the SKSac arrival (right): hence the arrival manifests a negative velocity contrast as imaged at 35-37° latitude in Fig. 4.

Deconvolution. Receiver functions are estimated via a multi-channel spectral deconvolution method that assumes pure mode (P-to-P or S-to-S) scattering is both minimum phase and non-zero so that three-component (P, S_V, S_H) receiver functions are calculated. The method has three fundamental steps. First, the P-component spectra from all stations recording each earthquake source are stacked and fit with a smooth spline to form an initial estimate of the source spectra. Second, the smooth estimates of the source spectra are used as constraint equations in a log-spectral least-

squares inversion to separate the amplitude spectra of the source and receiver functions. To exploit redundant sampling of similar source-receiver geometries, the sources recorded by each station are binned by ray parameter (0.0035 s/km) and back-azimuth (10°) so that a single estimate of the three-component receiver function is obtained for each bin. In the third step, the Kolmogorov spectral factorization is used to construct a set of sequential all-pass filters that recover the phase spectra of the source and receiver functions.

Common conversion point stacks of the Ps and Sp receiver functions produce images of the subsurface shear velocity contrasts. The migration velocity profiles for incident and converted raypaths are extracted through 3-D velocity models and used in the 1-D Ps/Sp moveout equation. This approximation does not perturb the raypaths calculated through the AK135 1-D reference velocity model nor is the incident ray parameter perturbed. For the shallow (<200 km) images, migration velocities are extracted from a 3-D SV surface wave velocity model (Shen and Ritzwoller, pers. com.) and a Vp/Vs of 1.76 (crust) and 1.81 (mantle) is assumed. For our deep (200-800 km) common conversion point images, migration velocities are extracted from a coupled P and S velocity tomogram (Schmandt and Humphreys, 2010).

Sp signal interpretation. Forward scattered P/S arrival amplitudes are dimmed towards zero when a velocity gradient is >1/2 wavelength of the dominate frequency of the incident wavelet (Bostock, 1999). Given a dominate 8 s period for our incident S-waves, significant Sp arrivals would require a velocity gradients < 17 km. Thus, observation of significant sub-moho negative polarity Sp arrivals in our images requires velocity gradients sharper than what an equilibrium geotherm across at the base of the thermal lithosphere can produce (Rychert et al., 2007). Hence it has been suggested that Sp negative arrivals require a hydration and/or partial melt porosity gradient at the base of the thermal lithosphere. The partial melt and hydration hypothesis are correlated because solid-state hydration partitions into the melt phase. To make a <17 km melt porosity gradient at the base of the thermal lithosphere depends on the evolution of the melt permeability tensor. A simple model to make a sharp melt porosity gradient is that small melt fluxes into the base of the lithospheric geotherm are thermally quenched to limit the upward flux of melt. Over time, as the lower lithosphere is warmed via melt fluxes and/or thinned by convective stresses, melt eventually reaches the surface via dykes as required by the abundant mantle xenoliths sampled by the New Mexico volcanic fields.

The taxonomy of sub-moho negative arrivals has two species at present: 1) a LAB arrival hypothesized to manifest the juxtaposition of melt/hydration gradients at the base of the thermal lithosphere; 2) a MLD (mid-lithosphere discontinuity) arrival hypothesized to manifest a sharp chemical contrast: e.g., a hydrated shallow mantle lithosphere overlying a dry thermally accreted lowermost lithosphere.

Beneath much of our sampling area, the primary Sp negative structure can be reasonably interpreted as a LAB arrival given the high-heat flow, young volcanic activity in the CRM, RGR, and along the Jemez volcanic lineament, and new evidence supporting the post 8-10 Ma acceleration of uplift of the CRM (Karlstrom et al., in review). Yet, interpretation of Sp negative arrivals in SE New Mexico and west Texas from the RISTRA (see McClenahan et al. poster) and SIEDCAR arrays (Fig. 4,5) presents a challenge. Both Rayleigh wave and body wave velocity tomograms image neutral to high velocity from the Moho to 150 km depth (Schmandt and Humphreys, 2010; Weisen and Ritzwoller, pers. com.). If one assumes that fast velocity manifests low temperatures, then interpreting the Sp negative arrivals as a LAB-signal seems implausible. Likewise, interpretation of a Sp negative arrival within the central Colorado Plateau sampled by the RISTRA array, where a high velocity upper mantle anomaly (the Escalante anomaly) extends to >150 km depth (Levander et al., 2011) presents a challenge to a LAB interpretation. Finally, a deep secondary Sp negative at 160 km depth is found in both the Big-line (Fig. 4) and RISTRA images (McClenahan et al. meeting abstract). We speculate this Sp negative arrival represents a melt porosity band produced by crossing of the wet mantle solidus due to an upwelling hydrous diapir from a partially molten 410 km discontinuity low velocity layer (Youngs and Bercovici, 2008) that is resolved by our deep Ps images not presented herein (Zhang and Dueker, pers. com.).

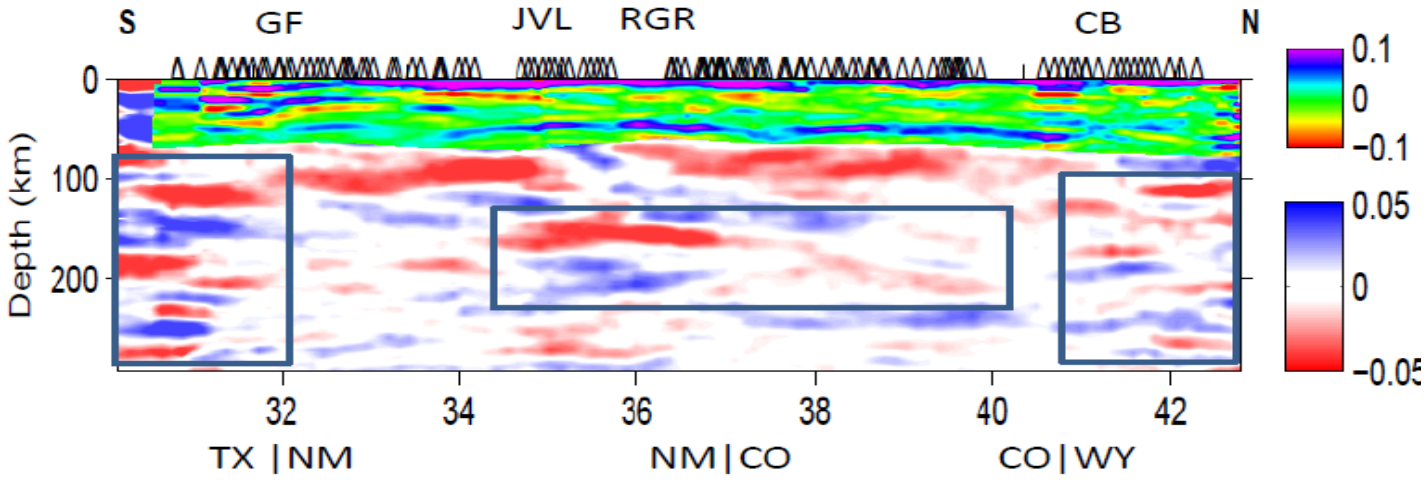

Figure 4. 'Big-Line' Sp/Ps common conversion point image that combines CREST, SIEDCAR, CDROM, and TA data. The upper 80 km image is from Ps data and the rest of the image is from Sp data. Cross section line shown in Fig. 5. Labels are: 1.1 Ga Grenville Front suture (GF), Jemez volcanic lineament (JVL), Rio Grande Rift (RGR), and 1.8 Ga Cheyenne belt suture (CB), Texas (TX), New Mexico (NM), Colorado (CO), Wyoming (WY). The middle box outline the deep Sp negative strongest under the JVL/RGR area and the outer boxes show where the shallow Sp structure changes across the GF and CB pre-Cambrian sutures.

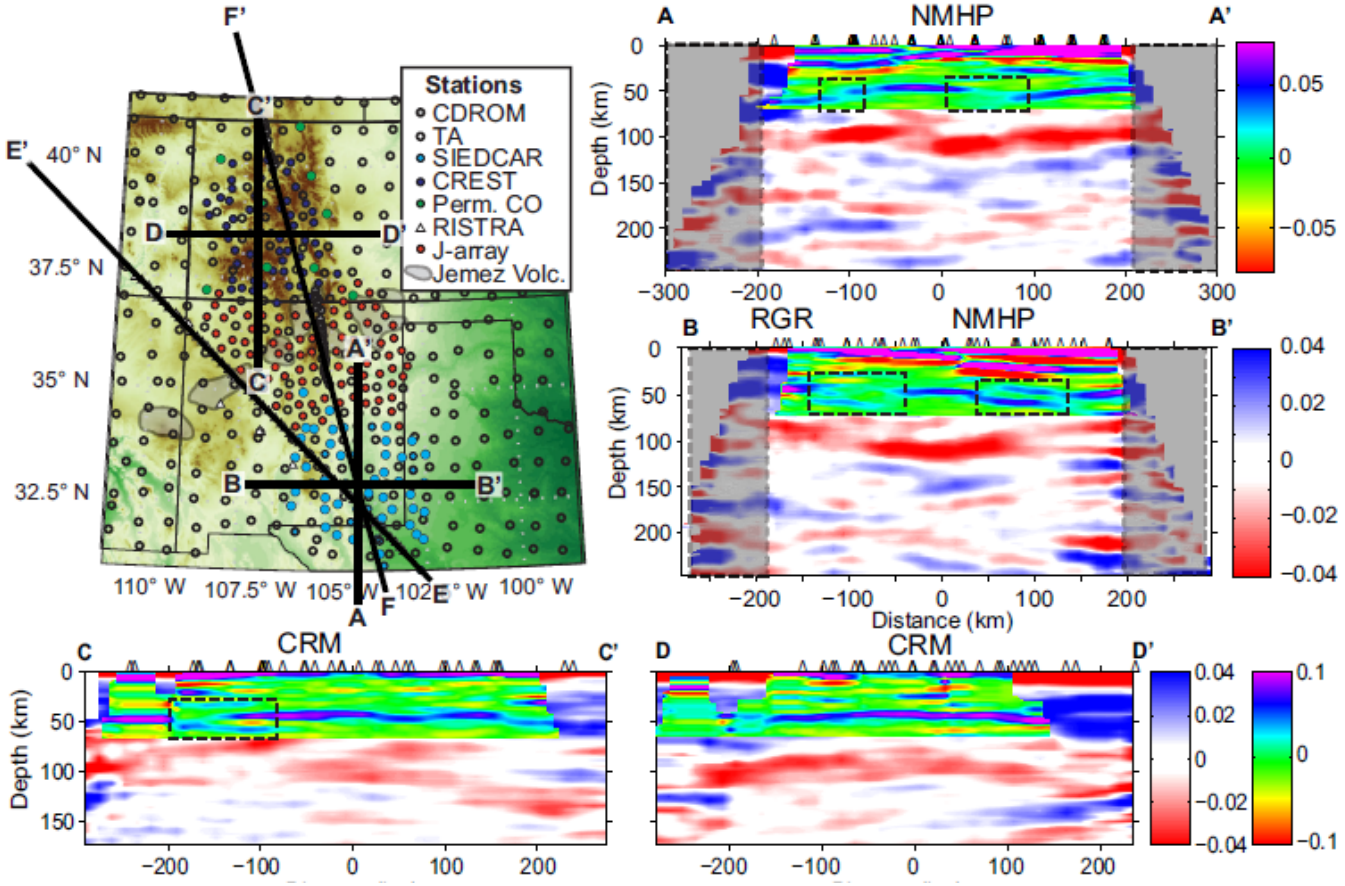

Figure 5. Ps/Sp cross-sections through the CREST and SIEDCAR arrays. The upper 80 km image is from Ps data and the rest of the image is from Sp data. Labels are: Rio Grande Rift (RGR), Colorado Rocky Mountains (CRM), New Mexico High Plains (HMHP). Cross section F-F' is called the Big-line (Fig. 4) and section E-E' is shown in the McClenahan et al. meeting abstract. The dotted boxes over the Ps image show moho doublets, imbrications and dim-out features.